Deep Learning Based Steel Pipe Weld Defect Detection

Dingming Yang, Yanrong Cui, Zeyu Yu & Hongqiang Yuan

Taylor & Francis
Taylor & Francis Group

Check for updates

Deep Learning Based Steel Pipe Weld Defect Detection

Dingming Yang [a], Yanrong Cui [a], Zeyu Yu [b], and Hongqiang Yuan[c]

[a]School of Computer Science, Yangtze University, Jingzhou, China; [b]School of Electronics & Information, Yangtze University, Jingzhou, China; [c]School of Urban Construction, Yangtze University, Jingzhou, China

ABSTRACT

Steel pipes are widely used in high-risk and high-pressure scenarios such as oil, chemical, natural gas, shale gas, etc. If there is some defect in steel pipes, it will lead to serious adverse consequences. Applying object detection in the field of deep learning to pipe weld defect detection and identification can effectively improve inspection efficiency and promote the development of industrial automation. Most predecessors used traditional computer vision methods applied to detect defects of steel pipe weld seams. However, traditional computer vision methods rely on prior knowledge and can only detect defects with a single feature, so it is difficult to complete the task of multi-defect classification, while deep learning is end-to-end. In this paper, the state-of-the-art single-stage object detection algorithm YOLOv5 is proposed to be applied to the field of steel pipe weld defect detection and compared with the two-stage representative object detection algorithm Faster R-CNN. The experimental results show that applying YOLOv5 to steel pipe weld defect detection can greatly improve the accuracy, complete the multi-classification task, and meet the criteria of real-time detection.

Introduction

Steel pipes are widely used in high-risk and high-pressure scenarios such as oil, chemical, natural gas, shale gas, etc. If there is some defect in steel pipes, it will lead to serious adverse consequences. With the growing demand for steel pipe in China, more and more enterprises and even countries begin to pay attention to the quality and performance of steel pipe, and the defect detection and evaluation technology of steel pipe has become a research topic that researchers are keen on. At present, there are manual testing and X-ray testing. X-ray testing is one of the main methods for industrial nondestructive testing (NDT), and the test results have been used as an important basis for defect analysis and quality assessment of weld. X-ray detection can effectively detect the internal defects of steel pipe, but manual participation is still needed to determine the type and location of weld defects of steel pipe (Yun et al. 2009).

Therefore, applying object detection in the field of deep learning to the defect detection and identification of steel pipe welds can effectively improve the detection efficiency and promote the development of industrial automation.

With the wide application of artificial intelligence in the field of computer vision, machine learning and deep learning are widely used in object detection and image classification. Most predecessors used traditional computer vision methods to detect steel pipe weld defects (Malarvel and Singh 2021; Wang et al. 2008; Yun et al. 2009). For example, Malarvel and Singh (2021) used OSTU + MSVM-rbf (Multi–class Support Vector Machine) method to achieve multi-class detection of weld defects in X-ray images and achieved an accuracy of 95.23%. Nowadays, object detection algorithms based on deep learning are constantly developing, and the recognition accuracy and detection time have been greatly improved compared with traditional computer vision methods. For example, Xiaojun Wu et al. (2021) used GAN (Generative Adversarial Network) to expand the insufficient defect data sets and proposed CFM (Coarse-to-Fine Module) to improve the segmentation algorithm with a good result; Yanqi Bao et al. (2021) proposed TGRNet (Triplet-Graph Reasoning Network) for metal generic surface defect segmentation and achieved good results. Previous studies have achieved good results, but there are also some shortcomings, such as:

- Accuracy rate needs to be further improved;
- Different types of defects make it difficult to do multiple classifications with traditional computer vision methods;
- Detection time is too long to achieve real-time detection, so it is difficult to apply to the industrial field;

In view of the above problems, this paper applies the state-of-the-art YOLOv5 to the defect detection task of steel pipe weld.

Materials and methods

Profile of YOLOv5

Joseph Redmon et al. (2016a) published YOLOv1 in 2015, which pioneered the single-stage object detection algorithm. This algorithm divides images into 7*7 grids, and each grid is responsible for the classification of objects and coordinate regression at the same time. Redmon and Farhadi (2016b) published YOLO9000 in 2016 to make up for the shortcoming of YOLOv1 with fewer detection categories and low accuracy, but the detection of small targets is still poor. Redmon and Farhadi (2018) published YOLOv3 in 2018, which draws on the idea of FPN (Tsung-Yi Lin et al. 2017), and solves the detection problem of small objects. Alexey Bochkovskiy, Wang, and Liao (2020)
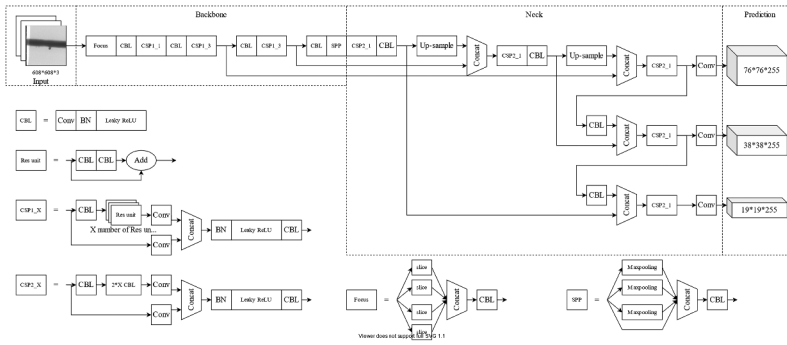
Figure 1. Network structure of YOLOv5s.

improved their algorithm by absorbing the tricks of various fields on the basis of the network structure of YOLOv3 and released YOLOv4, which greatly improved the detection efficiency and AP. Two months later, Ultralytics (a company) released YOLOv5 (Jocher et al. 2021).

According to the size of the model, YOLOv5 is divided into four versions: YOLOv5s, YOLOv5m, YOLOv5l, and YOLOv5x. The larger the model is, the higher the accuracy will be, and the detection time of a single image will increase. Figure 1 shows the network structure of YOLOv5s. The technologies used in the Input of YOLOv5 include Mosaic data enhancement (Yun et al. 2019), adaptive anchor calculation, and adaptive image scaling. The technology used in Backbone includes Focus structure and CSP structure. The techniques used in Neck include FPN+PAN structure. In Prediction, GIoU_Loss (Hamid Rezatofighi et al. 2019) is used to replace the ordinary IoU calculation method. YOLOv5 is slightly less capable than YOLOv4 in terms of performance, but much more flexible and faster than YOLOv4, so it has an advantage in model deployment.

Image acquisition device

The real-time X-ray imaging system used in this paper is shown in Figure 2. The system mainly consists of a welded pipe moving part, HS-XY-225 X-ray machine, PS1313DX high-speed digital panel detector, image capture card, and display part. In the welded pipe moving part, the spiral submerged arc welded pipe is moved using a transmission vehicle with four longitudinal rollers fixed on the vehicle for rotating the spiral submerged arc welded pipe. The X-ray machine is fixed to the wall on one side and deep into the pipe on the other side, emitting X-rays that penetrate the weld seam. A flat panel detector absorbs the X-ray photons that pass through the weld, creating electronic data that retains information on the attenuation of the photons. An
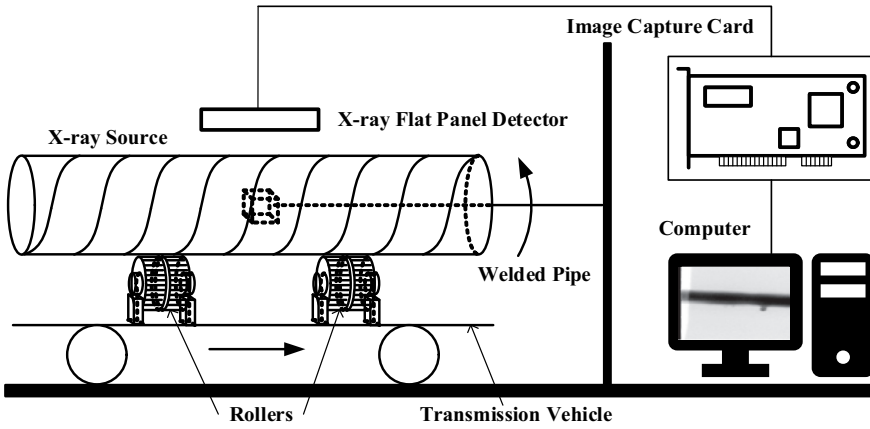
Figure 2. The real-time X-ray imaging system.

image capture card is used to convert the electronic data into a digital image sequence, which is then transferred to a computer for processing and display. Limited to hardware performance, only eight X-ray images per second can be captured and processed.

Acquisition of dataset

The raw video images of X-ray are provided by the cooperating factories in RAW format using the real-time X-ray imaging system in Figure 2. Through batch processing, the same width and height are cut out and exported as JPG images, and 3408 original images of weld defects of eight types of steel pipe are obtained. Finally, Labelme (a software to mark object) was used to mark the defect area and defect category of steel pipe weld, which was then exported as the standard dataset format of YOLO or PASCAL VOC2007 (Ren et al. 2017).
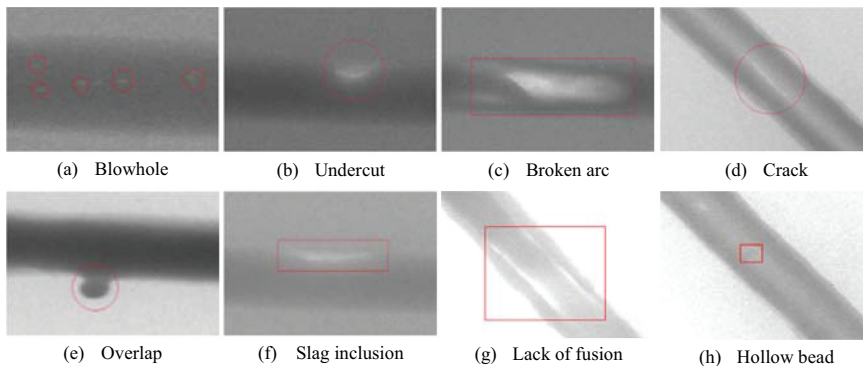

Figure 3. The example of steel pipe defects.

**Table 1.** Profile of sample images for eight types of defects.

Defect name	Number of original samples	Number of augmented samples	Label
Blowhole	1339	12051	Blow-hole
Undercut	35	315	Undercut
Broken arc	531	4779	Broken-arc
Crack	119	1071	Crack
Overlap	219	1971	Overlap
Slag inclusion	136	1224	Slag-inclusion
Lack of fusion	416	3744	Lack-of-fusion
Hollow bead	613	567	Hollow-bead
Totals	3408	30672	– –

Figure 3 shows the types of steel pipe weld defects. The collected samples have a total of eight types of defects, which are Blowhole, Undercut, Broken arc, Crack, Overlap, Slag inclusion, Lack of fusion, and Hollow bead. Table 1 shows the statistical table of steel pipe weld defects samples.

Data preprocessing

Raw dataset analysis

First of all, the original data should be analyzed so as to serve as a reference when setting parameters for deep learning and to accelerate the training speed. It can be seen from observation that X-ray pictures are black and white pictures, which can be converted into single-channel grayscale images. In this way, 2/3 pixels data can be compressed, and the training speed will be accelerated. We then use Matplotlib (a python lib to draw diagram) to draw the scatter plot of the center point position of the bounding box and the length and width of the bounding box in turn to see if there are any extreme aspect ratios and abnormal data. As shown in Figure 4, it can be concluded that most bounding boxes are wider than their height and that the bounding boxes for cracked defects are close to a square. Secondly, the displacement of most defects is in the horizontal direction, and the displacement of Overlap defects is from the bottom right to the top left. The distribution of scatter is more even, and there are not many abnormal data.
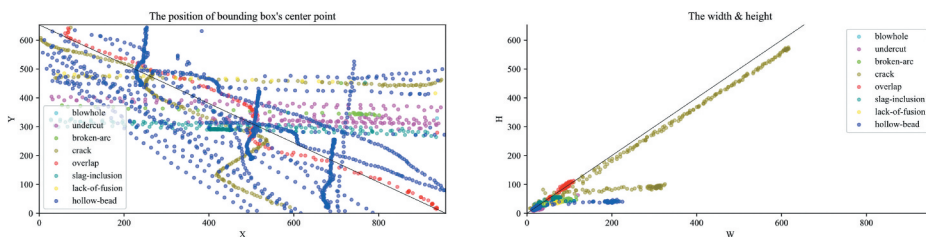
Figure 4. The analysis of original samples.

Motion deblurring

As shown in Figure 2, when the cylindrical steel pipe rotates in the assembly line, there will be relative movement between the X-ray camera used to film the weld defects of the steel pipe and the steel pipe in the direction of the weld. Moreover, the exposure time of the camera to shoot a single frame of weld defects is too long, so the motion blur will be generated. According to the research of Kupyn et al. (2018), motion blur will have an impact on the accuracy of object detection algorithm of YOLO series, so it is necessary to remove motion blur in some images. The process of motion deblurring is shown in Figure 5. First of all, we use the Hough Transform to detect the straight line at the weld edge. The direction of motion of the steel pipe can be estimated from the angle of the straight line (that is, the angle of image blur), and the distance of motion blur can be obtained from the frame rate of the camera and the speed of the steel pipe rotation. Then, we used the estimated blurry kernel for deconvolution of the original blurry image to get the result in Figure 5c.

Data enhancement

Convolutional neural network (CNN) usually requires a large number of training samples to effectively extract image features and classify them. In order to effectively improve data quality and increase data feature diversity, the original data was enhanced to nine times the original data by using light change, random rotation, random cut out, Gaussian noise addition, horizontal flipping, random adjustment of saturation, contrast and sharpness, random resize, and random clipping. Thus, the over-fitting in the training stage is effectively reduced, and the generalization ability of the network is improved. Figure 6 shows an example of what happens after data enhancement.

Experiments

Experimental environment

Tables 2 and 3 are the hardware environment and software environment of the experiment in this paper.
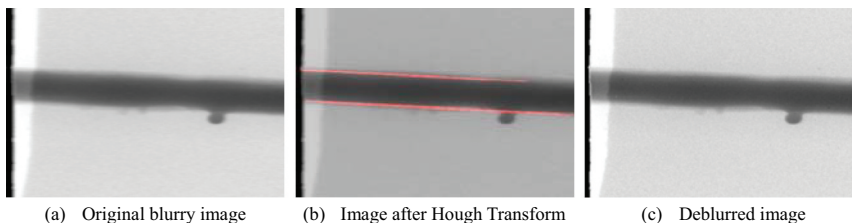

(a) Original blurry image   (b) Image after Hough Transform   (c) Deblurred image

Figure 5. The process of blind motion deblurring.

(a) Original image
(b) Image after change light
(c) Image after rotate
(d) Image after cutout
(e) Image after gaussian noise
(f) Image after horizontal flip
(g) Image after adjust color
(h) Image after resize
(i) Image after crop
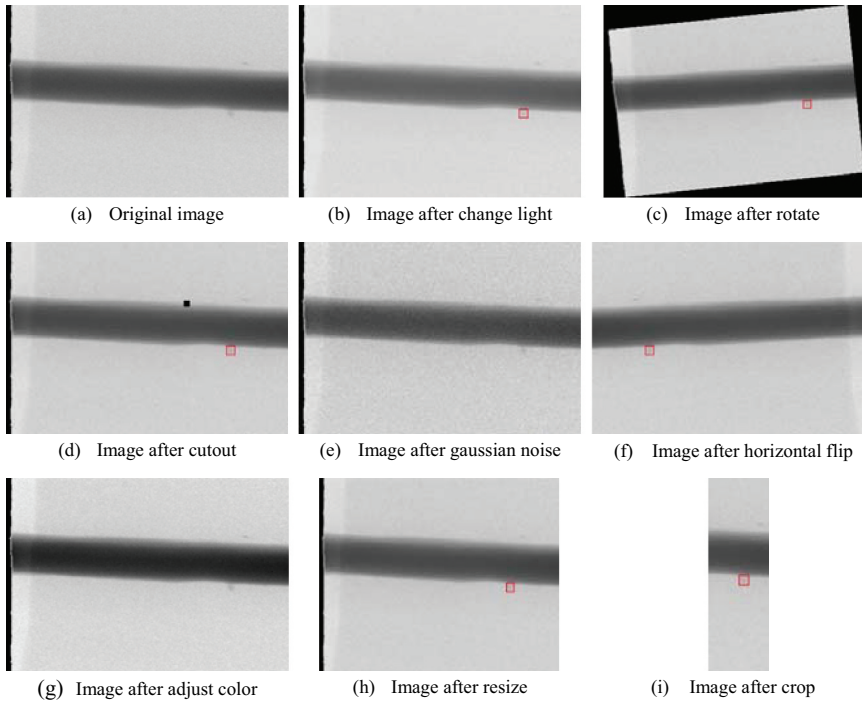
Figure 6. The example after data augmentation.

Table 2. The environment of hardware.

Phase	CPU	GPU	RAM
Train	Intel(R) Xeon(R) CPU E5-2623 v4 @ 2.60 GHz	Quadro P5000	30 GB
Test	Intel(R) Core(TM) i7-4710MQ CPU @ 2.50 GHz	GTX950M	8 GB

Table 3. The environment of software.

Phase	OS	Python	Model
Train	Linux-5.4.0–65-generic-x86_64-with-glibc2.10	3.8.5	Official YOLOv5x
Test	Windows 10 professional edition	3.8.0	Official YOLOv5x

Experimental process

In this paper, the state-of-the-art deep learning algorithm YOLOv5 is used to train the detection model of steel pipe weld defects. After manually annotating the original image, the dataset is obtained through data enhancement, and then, the dataset is converted into a single-channel grayscale image. Because the dataset is relatively small, it is divided into training set and validation set in a ratio of 8:2. An experimental process designed in this paper is shown in Figure 7. After several epochs of YOLOv5 training, the training set and
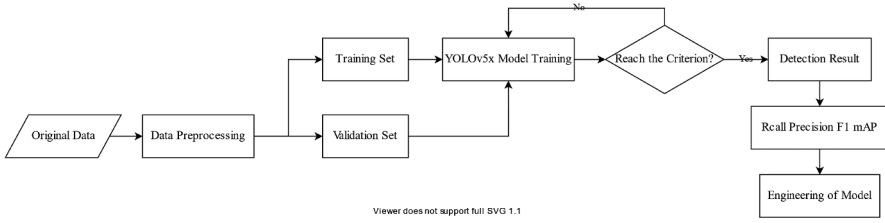
Figure 7. The flowchart of experiment.

validation set obtained a model containing weight and bias parameters. In this paper, Recall, Precision, F1 score, mAP (mean of Average Precision), and detection time of single image were used as evaluation indexes.

The calculation method of Precision is shown in Formula (1). TP is the sample identified as true positive. In this paper, it is the identification of correct weld defects of steel pipe. FP is the sample identified as false positive. In this paper, it is the weld defect of steel pipe identified wrongly. The formula describes the proportion of true positive in the identified pictures of steel pipe weld defects. The calculation method of Recall is shown in Formula (2). FN is the sample identified as false negative and in this paper is the background of error identification. The formula describes the ratio of the number of correctly identified steel pipe weld defects to the number of all steel pipe weld defects in the dataset. The calculation method of F1 score is shown in Formula (3). When Precision and Recall are required to be high, F1 score can be used as an evaluation index. The calculation method of AP is shown in Formula (4). AP is introduced to solve the problem of limitation of Precision, Recall, and F1 score single point value. In order to obtain an indicator that can reflect the global performance, in this paper, we use the interpolated average precision.

$$\text{Precision} = \frac{TP}{TP+FP} \tag{1}$$

$$\text{Recall} = \frac{TP}{TP+FN} \tag{2}$$

$$F_1 = \frac{2*Precision*Recall}{Precision+Recall} \tag{3}$$

$$P_{\text{interp}}(k) = \max_{\hat{k} \geq k} P(\hat{k})$$
$$AP = \sum_{k=1}^{N} P_{\text{interp}}(k)\Delta r(k) \tag{4}$$

(a) Blowhole (b) Undercut (c) Broken arc (d) Crack

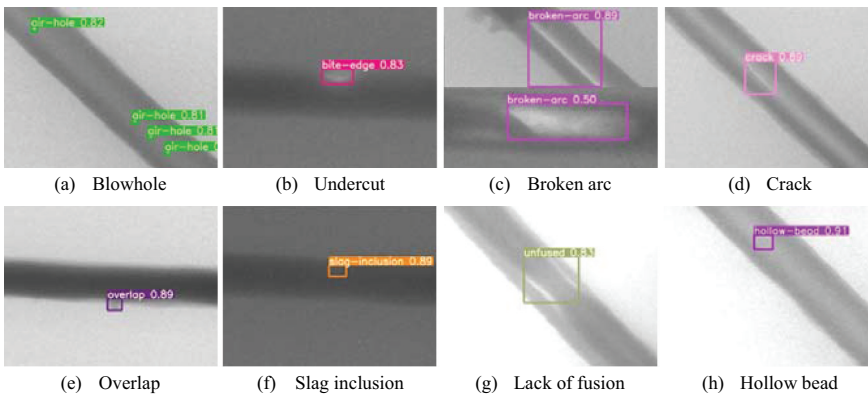(e) Overlap (f) Slag inclusion (g) Lack of fusion (h) Hollow bead

Figure 8. The result of detection.

Analysis of experimental results

Identify results and data analysis

The detection result for eight types of defects is shown in Figure 8. On the whole, both the position of defects and the confidence of classification are relatively good. Undercut's good performance in the case of a relatively small number of samples could not be attributed to the eight data enhancement methods used in the data preprocessing stage of this paper and Mosaic data enhancement by YOLOv5. The Broken can still be identified as the same defect and obtain good confidence even if they are very different in appearance. Among them, the Slag inclusion defects are not obvious to distinguish from the background in the naked eye, and they are similar to the Undercut defects in appearance. Benefiting from repeated training, good results can also be achieved.

As shown in Table 4, four evaluation indexes of each defect category in the last epoch are presented. On the whole, except for Blowhole defect, the accuracy of all other defects can be maintained between 0.962 and 1.00, the recall rate between 0.99 and 1.00, and the F1 score between 0.998 and 1.00. Blowhole defect due to its small defect target, a single steel pipe sometimes has

Table 4. Some statistical parameters of confusion matrix.

Type	Blowhole	Undercut	Broken-arc	Crack	Overlap	Slag-inclusion	Lack-of-fusion	Hollow-bead
Precision	0.505	1.00	0.962	1.00	1.00	1.00	0.99	0.99
Recall	0.96	1.00	1.00	1.00	1.00	1.00	0.99	1.00
F1 score	0.661	1.00	0.98	1.00	1.00	1.00	0.99	0.994
AP	0.951	0.995	0.995	0.992		0.995	0.995	0.995
	0.978							
mAP@0.5	0.987							

dense pores, so the accuracy is lower than other types of defects. In the 218th epoch, the mAP of the model reached 99.02%, but after 633 epochs of training, the mAP decreased to 98.71%, showing some degree of over-fitting. The best training model saved in this paper can be used in the actual steel pipe weld defect detection and applied in the industrial production environment.

Performance comparison of weld defect detection algorithm for steel pipe

As shown in Figure 9, we used the same dataset to conduct experiments, respectively, in Faster R-CNN (Bubbliiiing 2020; Ren et al. 2017) and YOLOv5 (Jocher et al. 2021) and then compared the precision data and total loss data generated during the experiment. As shown in Figure 9a, Faster R-CNN calculates the precision mean after each epoch of training and has a tendency of descending and then slowly climbing, with unstable values in the second half. YOLOv5, on the other hand, started off with a shaky precision and then slowly climbed up and settled down. As shown in Figure 9b, the total loss of Faster R-CNN tended to be stable between 50 and 100 epochs and then had two relatively large wave peaks. Since Faster R-CNN uses the Adam (Kingma and Jimmy 2014) optimizer, it can converge faster than SGD (Stochastic Gradient Descent). The initial total loss of YOLOv5 was relatively small and tended to be stable between 100 and 150 epochs, with a small peak around 160 epochs. YOLOv5 also uses the optimizer Adam, and the initial value of Momentum is 0.999. In general, compared with the Faster R-CNN, YOLOv5 has better convergence speed in precision and total loss and stability after convergence than the Faster R-CNN.
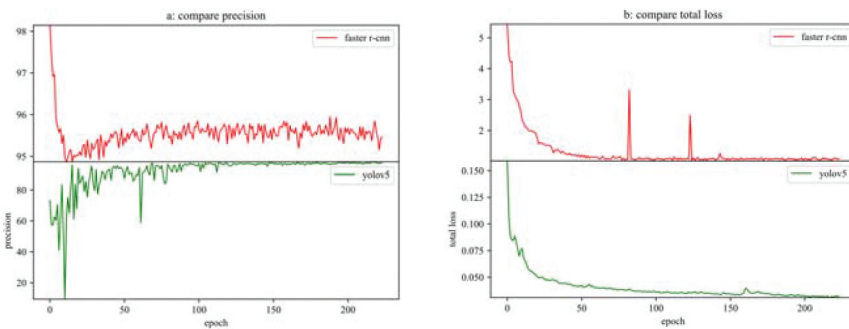

Figure 9. Comparison with faster R-CNN.

Table 5. Performance comparison of steel pipe detection algorithms.

Object detection model	Accuracy or precision/%	Detection time per picture/s
GAN+CFM (Wu et al. 2021)	85.9 acc (mIoU)	0.132
OSTU+MSVM-rbf (Malarvel and Singh 2021)	95.23 acc	– –
Faster R-CNN+ResNet50 (Ren et al. 2017)	95.5 acc (mAP@0.5 = 78.1)	0.437
YOLOv5x	97.8 pre (mAP@0.5 = 98.7)	0.120

As shown in Table 5, a comparison is made between GAN+CFM, OSTU +SVM, Faster R-CNN+ResNet50, and YOLOv5. On the whole, the defect detection algorithm based on deep learning is better than the defect detection algorithm based on traditional computer vision in both performance and detection time of a single image. Among them, GAN+CFM algorithm takes the longest time; OSTU+MSVM-rbf algorithm has the lowest accuracy. YOLOv5 is superior to Faster R-CNN in both accuracy and detection time of a single image. The detection time of a single image satisfies the engineering work of the model in the later stage of this paper. YOLOv5's detection speed is to be expected because it is one stage. Another kind of object detection algorithms is two stages. For example, the Faster R-CNN algorithm forms region proposals (which may contain areas of the object) first and then classifies each region proposal (also corrects the position at mean time). This type of algorithm is relatively slow because it requires multiple runs of the detection and classification process.

Conclusion

In the field of steel pipe weld defect detection, deep learning method has more advantages than traditional computer vision method. Convolutional neural network does not need to extract image features manually and can realize end-to-end input detection and classified output. The research of this paper has the following three contributions:

- Applying the state-of-the-art object detection algorithm YOLOv5 to the field of steel pipe weld defects detection, the detection accuracy of steel pipe weld defects and the detection time of a single image are pushed to a new height level, with the accuracy reaching 97.8% (mAP@0.5 = 98.7%). Under the YOLOv5x model testing, the detection time of a single picture is 0.12 s (GPU = GTX950M), which meets the real-time detection on the steel pipe production line;
- Did a lot of work in the data preprocessing stage, combining the traditional data enhancement method with the Mosaic data enhancement method of YOLOv5, which not only greatly increased the size of the dataset but also effectively reduced the over-fitting of the training;
- The results of YOLOv5 were compared with previous defect detection algorithms, and the advantages of YOLOv5 in model deployment and model engineering were demonstrated on the premise of comprehensive indicators.

This study can provide methods and ideas for real-time automatic detection of weld defects of steel pipe in industrial production environment and lay a foundation for industrial automation. Although this paper uses state-of-the-

art deep learning algorithm and convolutional neural network model for real-time detection of steel pipe weld defects in industrial production scenarios, its performance is also relatively good. However, in the case of limited dataset, other defects which are not in the dataset cannot be correctly identified. In this case, we can use traditional computer vision or mathematical methods to build an expert system to identify other defects that do not appear in the dataset. It is also possible to design an automatic updating model system in combination with Few-shot learning in engineering, which is used to manually label the type and bounding box coordinate information by the quality inspector when the defect cannot be identified, so that the system can automatically learn and update the model. These deficiencies point out the direction and provide ideas for the follow-up research.

Disclosure Statement

Funding

ORCID

Dingming Yang http://orcid.org/0000-0003-4555-4202
Yanrong Cui http://orcid.org/0000-0001-7903-6441
Zeyu Yu http://orcid.org/0000-0001-7430-9092

Supplemental Online Material

The dataset of steel pipe weld defect; Data during experiment; Figure 1. Network structure of YOLOv5s; Figure 3. The analysis of original samples; Figure 6. The flowchart of experiment; Figure 8. Comparison with faster R-CNN.

Author Contributions

Conceptualization, D.Y., Y.C., and Z.Y.; Software, D.M., Resources, Z.Y., H.Y.; Supervision, Y.C., Z.Y.; Writing – original draft, D.Y.; Writing – review and editing, D.Y., Y.C., and Z.Y. All authors have read and agreed to the published version of the manuscript.

References

Bao, Y., K. Song, J. Liu, Y. Wang, Y. Yan, H. Yu, and X. Li. 2021. Triplet-graph reasoning network for few-shot metal generic surface defect segmentation. *IEEE Transactions on Instrumentation and Measurement* 70:1–11. doi:10.1109/TIM.2021.3083561.

Bochkovskiy, A., C.-Y. Wang, and H.-Y. M. Liao. 2020. YOLOv4: optimal speed and accuracy of object detection. *arXiv Preprint arXiv* 2004:10934.

Bubbliiiing. Faster-Rcnn: implementation of two-stage object detection model in tensorflow2. Accessed December 1, 2020. https://github.com/bubbliiiing/faster-rcnn-tf2 .

Jocher, G., K. Nishimura, T. Mineeva, and R. Vilariño. YOLOv5. Accessed March 1, 2021. https://github.com/ultralytics/yolov5 .

Kingma, D., and B. Jimmy. 2014. Adam: a method for stochastic optimization. *arXiv Preprint arXiv* 1412:6980.

Kupyn, O., Budzan, V., Mykhailych, M., Mishkin, D., and Matas, J. 2018. DeblurGAN: Blind Motion Deblurring Using Conditional Adversarial Networks. 2018 IEEE/CVF Conference on Computer Vision and Pattern Recognition, Salt Lake City, UT, USA, (pp. 8183–8192). doi:10.1109/CVPR.2018.00854.

Lin, T.-Y., P. Dollár, R. Girshick, H. Kaiming, B. Hariharan, and S. Belongie. 2017. Feature pyramid networks for object detection. *arXiv Preprint arXiv* 1612:03144.

Malarvel, M., and H. Singh. 2021. An autonomous technique for weld defects detection and classification using multi-class support vector machine in X-radiography image. *Optik* 231:166342. doi:10.1016/j.ijleo.2021.166342.

Redmon, J., and A. Farhadi. 2016b. YOLO9000: Better, faster, stronger. *arXiv Preprint arXiv* 1612:08242.

Redmon, J., and A. Farhadi. 2018. YOLOv3: an incremental improvement. *arXiv Preprint arXiv* 1804:02767.

Redmon, J., S. Divvala, R. Girshick, and A. Farhadi. 2016a. You only look once: unified, real-time object detection. *arXiv Preprint arXiv* 1506:02640.

Ren, S., K. He, R. Girshick, and J. Sun. 2017. Faster R-CNN: Towards real-time object detection with region proposal networks. *IEEE Transactions on Pattern Analysis and Machine Intelligence* 39 (6):1137–49. doi:10.1109/TPAMI.2016.2577031.

Rezatofighi, H., N. Tsoi, J. Gwak, A. Sadeghian, I. Reid, and S. Savarese. 2019. Generalized intersection over union: A metric and a loss for bounding box regression. *arXiv Preprint arXiv* 1902:09630.

Wang, Y., Y. Sun, P. Lv, and H. Wang. 2008. Detection of line weld defects based on multiple thresholds and support vector machine. *Ndt & E International* 41 (7):517–24. doi:10.1016/j.ndteint.2008.05.004.

Wu, X., L. Qiu, X. Gu, and Z. Long. 2021. Deep learning-based generic automatic surface defect inspection (ASDI) with pixelwise segmentation. *IEEE Transactions on Instrumentation and Measurement* 70:1–10. doi:10.1109/TIM.2020.3026801.

Yun, J. P., S. Choi, J.-W. Kim, and S. W. Kim. 2009. Automatic detection of cracks in raw steel block using Gabor filter optimized by univariate dynamic encoding algorithm for searches (uDEAS). *Ndt & E International* 42 (5):389–97. doi:10.1016/j.ndteint.2009.01.007.

Yun, S., D. Han, S. J. Oh, S. Chun, J. Choe, and Y. Yoo. 2019. CutMix: Regularization strategy to train strong classifiers with localizable features. *arXiv Preprint arXiv* 1905:04899.